 ISSN 0267-8179. DOI: 10.1002/jqs.1455

Late Pleistocene snowline fluctuations at Nevado Coropuna (15°S), southern Peruvian Andes

GORDON R. M. BROMLEY,[1]* BRENDA L. HALL,[1] KURT M. RADEMAKER,[1] CLAIRE E. TODD[2] and ADINA E. RACOVTEANU[3]
[1] Department of Earth Sciences and the Climate Change Institute, Edward T. Bryand Global Sciences Center, University of Maine, Orono, ME 04469-5790, USA
[2] Department of Geological Sciences, Rieke Science Center, Pacific Lutheran University, Tacoma, WA 98447, USA
[3] Department of Geography and Institute of Arctic and Alpine Research, University of Colorado, Boulder, CO 80309, USA

Received 12 May 2010; Revised 7 September 2010; Accepted 27 September 2010

ABSTRACT: Deposits preserved on peaks in the southern Peruvian Andes are evidence for past glacial fluctuations and, therefore, serve as a record of both the timing and magnitude of past climate change. Moraines corresponding to the last major expansion of ice on Nevado Coropuna date to 20-25 ka, during the last glacial maximum. We reconstructed the snowline at Coropuna for this period using a combined geomorphic-numeric approach to provide a first-order estimate of the magnitude of late-Pleistocene climate change. Our reconstructions show that snowline was approximately 550-770 m lower during the last glacial maximum than during the late Holocene maximum, which ended in the 19th century, and ~750 m lower than today. While these values are similar to data from nearby Nevado Solimana, reconstructions from the neighbouring peak of Nevado Firura reveal a smaller snowline depression, suggesting the glacial response to climate forcing in the tropics is strongly influenced by non-climatic factors. These data constitute some of the first directly dated palaeo-snowline data from the arid tropics and suggest that the magnitude of the last glaciation in at least parts of the tropical Andes was similar to late-Pleistocene events at higher latitudes. Copyright © 2011 John Wiley & Sons, Ltd.

KEYWORDS: tropics; glacier; snowline; equilibrium-line-altitude; last glacial maximum.

Introduction

As the energetic powerhouse of the earth and the principal source of atmospheric water vapour, the tropics have huge potential to trigger or amplify climate changes on a global scale (Pierrehumbert, 1999; Clement *et al.*, 2001; Koutavas *et al.*, 2002). Resolving the timing and structure of tropical climate change remains a key challenge in palaeoclimate research, with implications for our understanding of the causes of ice ages and the mechanisms driving abrupt climate change. In contrast to CLIMAP (1981), which suggested tropical climate is inherently stable, a growing body of evidence indicates significant tropical-climate variability during the late Pleistocene (Mercer and Palacios, 1977; Thompson *et al.*, 1995, 1998; Baker *et al.*, 2001; Greene *et al.*, 2002; Quade *et al.*, 2008). However, estimates of the magnitude of late-Pleistocene tropical climate change remain poorly constrained (Smith *et al.*, 2008). For example, estimations of atmospheric cooling in the tropics during the last glacial maximum (LGM) range from 2°C in central Peru (Wright, 1983) to as much as 8°C on Huascarán, Cordillera Blanca, Peru (Thompson *et al.*, 1995), and 8.8°C in the Venezuelan Andes (Stansell *et al.*, 2007). Further uncertainty arises from the relatively poor age control of glacial events in the tropics. Despite recent research (Zech *et al.*, 2007, 2008; Blard *et al.*, 2009; Pigati *et al.*, 2008; Smith *et al.*, 2008, and references therein; Bromley *et al.*, 2009), the number of sites where both the timing and magnitude of snowline change are constrained remains insufficient to identify patterns in tropical climate.

A common approach to investigating the structure of past climate events is to reconstruct palaeo-snowlines [frequently, and in the context of this study, equated with the equilibrium-line altitude (ELA)] on glaciated or formerly glaciated peaks, as a proxy for mean atmospheric temperature (Benn *et al.*, 2005). These values then are compared to modern snowline altitudes with the offset between the two providing a measure of the corresponding temperature change. This approach has been applied to sites throughout the tropics (Porter, 2001), with researchers implementing a wide variety of methodologies (Benn *et al.*, 2005). However, whereas several reconstructions suggest that the magnitude of tropical snowline lowering during the LGM was broadly consistent with average global values (~700-1000 m; Porter, 1979; Clapperton, 1987; Osmaston, 1989; Rodbell, 1992), others do not. For example, Wright (1983) calculated snowline depressions of as little as 300 m on the Junin Plain (Fig. 1a), central Peru, whereas Mark *et al.* (2002) reported changes of only 150 m and 360 m for the Cordillera Vilcanota (Fig. 1a) and Quelccaya Ice Cap, southern Peru, respectively. This discrepancy could be interpreted as indicating steep spatial gradients due to local and/or regional effects (Mark *et al.*, 2005; Kull *et al.*, 2008). Benn *et al.* (2005), however, concluded that the high variability of existing snowline estimates is more likely the result of the different and/or inappropriate methods used, as well as inadequate dating control, rather than of real climate variability. If true, this represents a serious shortcoming of the Peruvian glacier record.

We used multiple methods to reconstruct LGM snowlines for three peaks in the semi-arid Pucuncho region, south-western Peru. Ongoing glacier retreat makes it difficult to determine modern snowline elevations against which the overall magnitude of post-LGM snowline change can be measured (Benn *et al.*, 2005). Therefore, we compared the LGM data to snowline values during the late-Holocene maximum (equated here to the 19th century; see below), when glaciers in Peru were last in a state of mass balance (Kaser, 1999; Licciardi *et al.*, 2009), to approximate the magnitude of late-Pleistocene snowline depression. By incorporating measurements of the long-term (~1950 AD) snowline and of regional temperature change during the 20th century (Vuille *et al.*, 2008), we then estimated snowline changes at Coropuna since the late-Holocene maximum, thereby providing an estimate of LGM snowline depression in south-western Peru relative to today. We compare the degree of snowline lowering in our study area to other tropical and higher-latitude records.

Geographic and climatic setting

Nevado Coropuna (6450 m; 15° 33'S, 72° 93'W) is a large andesitic stratovolcano located on south of the Pucuncho Basin

*Correspondence: Gordon R. M. Bromley, 437 Comer Geochemistry, Lamont-Doherty Earth Observatory, 61 Route 9W, Palisades, NY 10964-8000, USA.
E-mail: gbromley@ldeo.columbia.edu

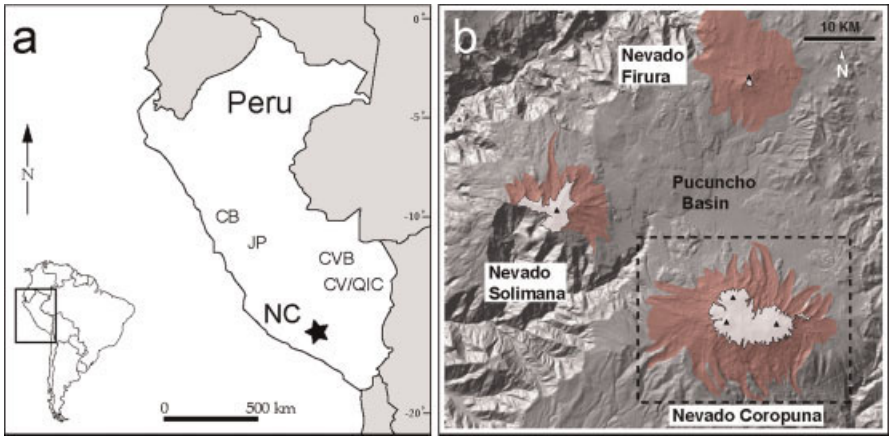

Figure 1. (a) Map of Peru showing locations of Nevado Coropuna (NC), the Cordillera Blanca (CB), the Junin Plain (JP), the Cordillera Vilcabamba (CVB), and the Cordillera Vilcanota/Quelccaya Ice Cap (CV/QIC); (b) The Pucuncho Basin and relative locations of Nevados Coropuna, Solimana, and Firura. White areas indicate modern ice cover. Shaded areas mark the extent of glaciers during the last glacial maximum (for reasons of access, we were unable to include the south side of Solimana in this study). Dashed box marks area in Figures 4 and 8. This figure is available in colour online at wileyonlinelibrary. com.

in the south-western Peruvian Andes, approximately 150 km north-west of Arequipa (Fig. 1, a and b). The volcano is in the northern sector of the Central Volcanic Zone and began forming during the late Miocene, though much of its present form is attributed to Quaternary volcanism (Venturelli *et al.*, 1978). The most recent activity occurred during the early Holocene, when three andesite flows emanated from the mountain (Venturelli *et al.*, 1978), in places overrunning moraines of late-glacial age (Bromley *et al.*, 2009). Due to the combined influences of the Andean rain shadow and a persistent temperature inversion over the Pacific coast, the prevailing climate at Coropuna is semi-arid, with most precipitation (~390 mm water equivalent per year at 6080 m; Herreros *et al.*, 2009) arriving during the summer wet season (December-March). The mountain comprises four high domes separated by broad saddles (Fig. 2) and supports an icecap of ~60.8 km^2 (Racoviteanu *et al.*, 2007). Outlet glaciers descend to ~5100 m on southern aspects but are restricted to elevations above ~5500 m on the mountain's north side.

The neighbouring peaks of Nevado Solimana (6093 m; 15°24'S, 72°52'W) and Nevado Firura (5498 m; 15°14'S, 72°48'W) are extinct, glaciated volcanoes located north-west and north of Coropuna, respectively (Fig. 1b). The larger of the two, Solimana, is of Miocene-Pliocene origin and was last active 0.3-0.5 Ma ago (Thouret *et al.*, 2007). Solimana owes much of its high-relief (~2000 m), alpine topography (Fig. 3a) to

Figure 2. The highest summit of Nevado Coropuna, seen from the south-west. The mountain comprises four principal domes, separated by broad saddles. This figure is available in colour online at wileyonlinelibrary.com.

Figure 3. (a) Nevado Solimana from the east, showing the peak's high-relief, alpine topography. The south-east face (in shadow) is ~400 m high. (b) South side of Nevado Firura, seen from the Pucuncho Basin, which has an elevation of ~4400 m at this location. This figure is available in colour online at wileyonlinelibrary.com.

subsequent glacial erosion of the collapsed caldera. Modern glaciers are restricted to the precipitous south-eastern face and to a shallow north-facing valley emanating from the former caldera. By contrast, Firura is a lower-relief (~500 m) complex (Fig. 3b) comprising two domes, rising from the high plateau north of the Pucuncho Basin. The higher (southern) summit exhibits a shallow cirque on its southern flank, occupied by a small (>0.5 km^2) glacier which flows down to 5255 m. Perennial snow covers much of the southern flank above ~5300 m, while the northern slope typically is bare.

Prominent, well-preserved lateral and end moraines occur on the lower slopes of all three peaks and attest to periods when glaciers were more extensive than at present. Bromley *et al.* (2009) described the Coropuna moraine record, while undated deposits on Solimana were discussed by Dornbusch (2002). There are no published accounts of glacial deposits on Firura. On Coropuna, recently published cosmogenic ^{3}He surface-exposure ages show that the largest moraines (as much as 100 m of relief) correspond to the last major expansion of glaciers during the LGM (Bromley *et al.*, 2009) (Fig. 4). Considering the proximity of the three peaks and the high degree of consistency among them in terms of moraine distribution and morphology, we have extrapolated the Coropuna chronology to cover Solimana and Firura. Figures 4–6 show the distribution of LGM glacial deposits on the three peaks.

On each mountain, series of fresh, grey moraines occur within 0.5 km of the modern glacier edge and mark the last stable position of the ice front. While there are no radiometric data for these late-Holocene moraines, extensive research in the Cordillera Blanca (10°S, Fig. 1a; Kaser, 1999; Solomina *et al.*, 2007) and the Cordillera Vilcabamba (13°S, Fig. 1a; Licciardi *et al.*, 2009) indicates that the last significant advance of glaciers in Peru ended during the early- to mid-19th century. We assume that the innermost prominent moraines on Coropuna, Solimana and Firura correspond to this period. Between these moraines and the glacier edge, small (<1-2 m high), discontinuous and commonly ice-cored mounds mark the recent and ongoing glacier recession.

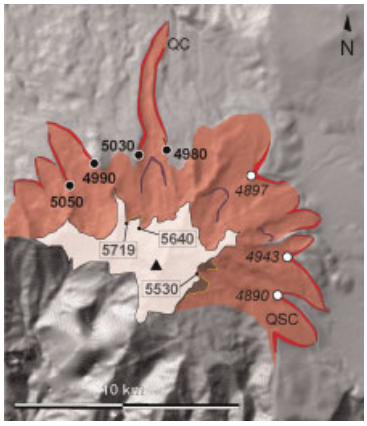

Figure 5. Distribution of glacial deposits on Solimana. White area indicates modern ice cover. For key to deposits see Figure 4. LGM MELM and bifurcation values, in metres, are given in bold and italics, respectively. Values given in boxes denote late-Holocene MELMs. MELM measurement locations are indicated by black circles, bifurcations by white circles. All elevations include ± 15 m GPS uncertainty. The south side of Solimana was not mapped as part of this study. Location names: QC - *Q.* Caño; QSC - *Q.* Saca Chacay. This figure is available in colour online at wileyonlinelibrary.com.

Midway between the 19th century deposits and the LGM termini, a complex of moraines marks an advance during the late-glacial period (Fig. 4) (Bromley *et al.*, 2009). A similar moraine stratigraphy occurs on both Solimana and Firura, suggesting the pattern of glacier events was regionally uniform. As we have not yet mapped the upper limits of these moraines in detail, late-glacial snowline reconstructions are not included here.

Owing in large part to the prevailing aridity, moraines on Coropuna, Solimana and Firura maintain prominent crests, steep slope morphology and clear upper limits. Vegetation cover below ~5000 m is sparse and dominated by Llareta (*Azorella compacta*) and ichu grass. Above ~5000 m, vegetation is absent.

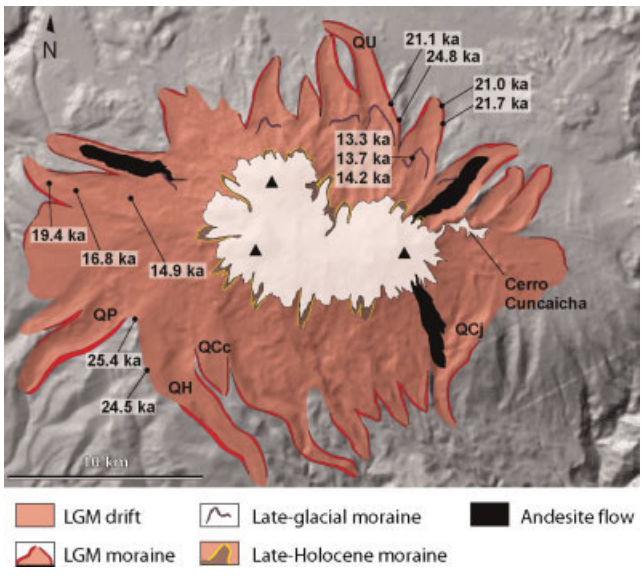

Figure 4. Cosmogenic ^{3}He ages from Nevado Coropuna (from Bromley et al., 2009). White area indicates modern ice cover. Location names: QU - *Q.* Ullullo; QP - *Q.* Pucunchiloyocc; QH - *Q.* Huayllaura; QCc - *Q.* Chipchane; QCj - *Q.* Cospanja. This figure is available in colour online at wileyonlinelibrary.com.

Methods

We reconstructed snowline elevations for the LGM and late Holocene using the maximum elevation of lateral moraines (MELM). As a direct consequence of net ice loss through melting and/or sublimation, deposition of lateral moraines occurs only below the snowline (Andrews, 1975). Consequently, the upper limits of lateral moraines afford an indication of former snowline elevations. Although this method has been used extensively (e.g. Rea *et al.*, 1999; Munroe and Mickelson, 2002; Asahi and Watanabe, 2004; Lachniet and Vazquez-Selem, 2005; Asahi, 2008), some (e.g. Meierding, 1982; Hawkins, 1985; Locke, 1990) have expressed concern that the derived reconstructions might underestimate true snowline as a result of moraine degradation. This effect likely is greatest in humid, high-relief environments (e.g. New Zealand) where erosion and slope processes are highly active. However, in arid environments, such as southern Peru, where the degree of landform preservation typically is high (Bromley *et al.*, 2009), the MELM method can provide an accurate first-order estimate of former snowline elevation (Benn *et al.*, 2005). MELM-derived reconstructions are especially valuable for sites like Coropuna where a dearth of mass-balance data precludes the application of other, more quantitative methods such as balance ratios. In addition to the MELM, we reconstructed

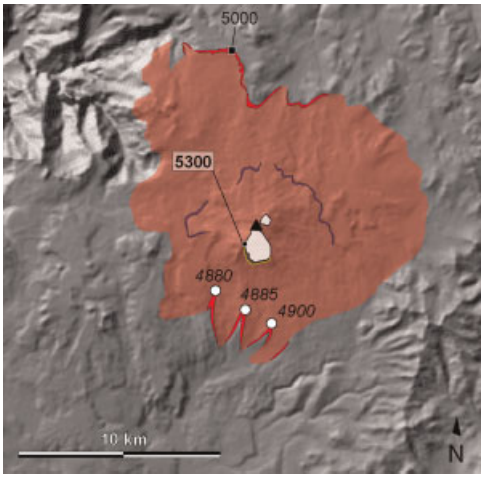

Figure 6. Distribution of glacial deposits on Firura. For key to deposits see Figure 4. White area indicates modern ice cover. LGM bifurcations are indicated by white circles. Values given in boxes denote late-Holocene MELMs. The highest point along the LGM terminal moraine (5000 m) is indicated by the black square. All elevations are given in metres and include ± 15 m GPS uncertainty. This figure is available in colour online at wileyonlinelibrary.com.

former snowlines using the toe-headwall-altitude-ratio (THAR) method in order to allow comparison of our datasets.

To determine the MELMs on Coropuna, Solimana and Firura accurately, we first mapped the distribution of glacial deposits onto enlarged aerial photographs in the field. We then constrained the maximum elevations of moraines with GPS measurements of 15 min duration, taken at the highest identifiable point on each landform. It is critical to differentiate between the upper limits of lateral moraines, which can indicate former snowline, and bifurcating moraines and moraines that terminate due to topography. Bifurcating moraines mark the division of former ice tongues into separate valleys below the snowline and afford only a minimum constraint on palaeo-ELA. Similarly, lateral moraines that end for topographic reasons (e.g. slopes too steep for moraine deposition) do not represent former snowline. To account for the vertical uncertainty of GPS measurements (estimated ± 15 m), all MELM measurements reported below include ± 15 m error. In addition, uncertainty values for averaged snowline elevations incorporate 1σ standard deviation of the mean propagated with the analytic GPS uncertainty in quadrature.

The THAR method assumes that the equilibrium line occurs at a set elevation between the terminus and head of a glacier (Meierding, 1982). To calculate LGM and late-Holocene snowlines, we employed a set of ratios between 0.2 and 0.3, considered by Osmaston (1975) and Kaser and Osmaston (2002) to be the most appropriate values for tropical volcanic domes and ice caps. In addition, we substituted the summit elevations for headwall values (Klein *et al.*, 1999). All ELA reconstructions presented here are based on field GPS measurements and, consequently are subject to an estimated uncertainty of ± 15 m. As with the MELM data, uncertainty values for averaged THAR-based snowlines incorporate 1σ standard deviation propagated with the analytic GPS uncertainty.

As we have no constraint of appropriate ratios for high-relief, alpine glaciers in this region, we present THAR-based reconstructions for Coropuna and Firura only. We compared the MELM- and THAR-based snowline reconstructions for Coropuna and Firura during the LGM and late Holocene. The derived values then were evaluated against MELM data from neighbouring Solimana.

Results

Maximum elevation of lateral moraines on Nevado Coropuna

Last Glacial Maximum MELMs

The most prominent moraines on Coropuna were deposited ~20-25 ka (Bromley *et al.*, 2009), during the LGM. On the mountain's north, west and south flanks, large lateral moraines grading into terminal moraines mark former outlet glacier extent. The largest glacier (12 km long) occupied north-flowing Quebrada (hereafter *Q.*) Ullullo (Figs. 4 and 7). On the eastern flank, a thin drift of boulders and cobbles overlying deeply weathered bedrock and older glacial deposits marks the former ice margin. LGM moraine crests on Coropuna typically are 5-10 m wide and dominated by sandy gravel and small boulders (<1 m high), though larger boulders (>1 m high) are common. Boulder surfaces are polished and striated.

Careful mapping of the landform distribution allows both reconstruction of former ice-cap configuration (Figs. 4 and 8) and identification of the upper limits of lateral moraines. During the LGM, the Coropuna ice cap covered an area of at least 365 km^2 and drained via outlet glaciers that descended as low as 4540 m on the north side and 3780 m on the south side. This represents an average lowering in terminus elevation of ~1000 m relative to today. MELMs are given in Table 1 and Fig. 8a. The highest MELM values occur on the north and east flanks and the lowest on the south. In north-flowing valleys, MELMs range from 5120 to 5230 m (mean 5167 ± 59 m; $n = 3$), and moraine bifurcations occur between 4930 and 5115 m ($n = 5$). Of the eight outlet glaciers draining Coropuna's south flank during the LGM, only two exhibit reliable MELMs: 4700 m in *Q.* Huayllaura and 4790 m in *Q.* Chipchane (mean 4745 ± 66 m; $n = 2$) (Fig. 8a). The upper limits of most lateral moraines on this slope form bifurcations ($n = 7$) (Table 1).

West-flowing glaciers deposited lateral moraines with upper limits between 4820 and 4970 m (mean 4887 ± 77 m; $n = 3$) (Fig. 8a). Several bifurcations also occur on this side of the mountain ($n = 4$) (Table 1). On the eastern flank, most ice flowing from Coropuna Este drained into *Q.* Cospanja (Figs. 4 and 8a) and was diverted south. Consequently, the LGM moraines on the eastern flank of Coropuna correspond to outlet

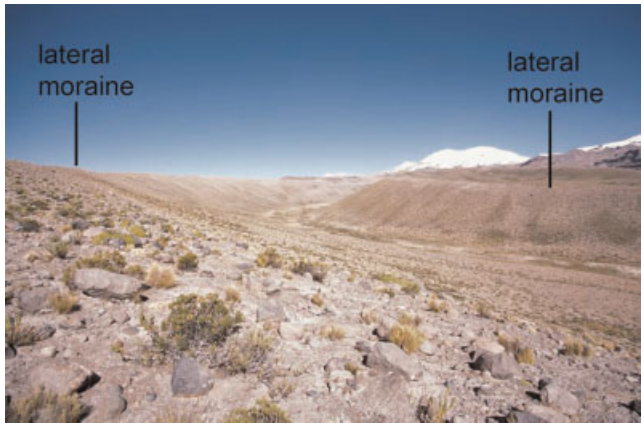

Figure 7. Large lateral-moraine ridges in Quebrada Ullullo, on the north side of Coropuna. Moraines shown are approximately 100 m in relief. Coropuna's eastern summit – Coropuna Este – is visible in the background. This figure is available in colour online at wileyonlinelibrary.com.

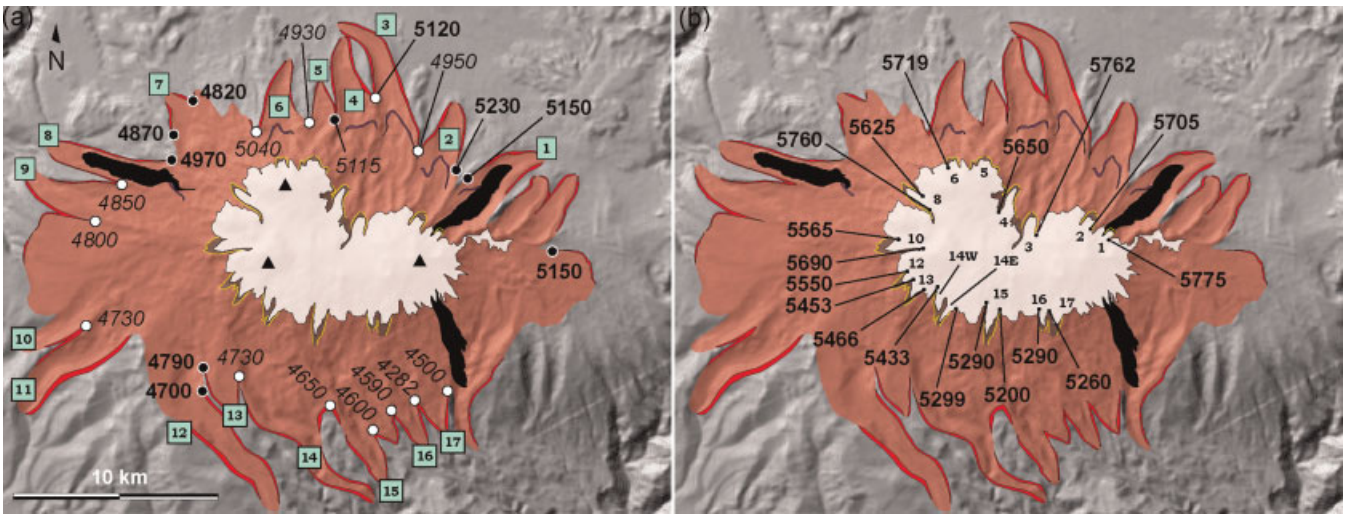

Figure 8. (a) Distribution of MELM (bold type) and bifurcation (italics) values, in metres, for the LGM on Coropuna. MELM measurement locations are indicated by black circles. Bifurcations are indicated by white circles. Glacier numbers mentioned in text and Table 2 are shown in boxes; (b) Distribution of late-Holocene MELM values. All elevations are subject to an estimated ± 15 m GPS uncertainty. Glaciers identified by numbers. This figure is available in colour online at wileyonlinelibrary.com.

glaciers of a small ice mass that accumulated on a spur (Cerro Cuncaicha) projecting from Coropuna Este. Lateral moraines deposited by these glaciers exhibit abrupt upper limits between 5010 and 5050 m ($n = 3$). As these limits occur at a significant change in slope angle, they are unlikely to represent former snowline and, thus, are not considered further. However, a lateral moraine on the gentle south side of Cerro Cuncaicha exhibits a clear upper limit at 5150 m.

Lateral moraines on Solimana indicate that long, narrow outlet glaciers drained the peak during the LGM (Fig. 5). The longest of these occupied *Q.* Caño (Fig. 5) and extended 9 km from near the mountain's summit to a terminus at 4530 m. Two large (>100 m relief) lateral moraines exhibit clear upper limits on gentle slopes at 4980 m (left lateral) and 5030 m (right lateral). A similar pair of landforms exhibits maximum elevations of 4990 m (left) and 5050 m (right) in a neighbouring valley (Table 1).

North of the Pucuncho Basin, the distribution of LGM moraines on Firura (Fig. 6) precludes accurate application of the MELM method. Ice flowing from this small volcano onto the surrounding plateau deposited a large (80-100 m relief), nearly continuous terminal moraine. At its highest point on the plateau (5000 m), this moraine lies only ~498 m below the summit. Where north-flowing ice intercepted two minor drainages, former terminus elevations are 4770 m and 4795 m (Fig. 6). Lateral moraines on Firura are rare and none affords a reliable MELM measurement. On the south flank, bifurcations corresponding to three outlet glaciers occur between 4880 and 4900 m (Table 1; Fig. 6).

Late-Holocene MELMs

A suite of fresh moraines, typically comprising two nested lateral-frontal ridges, occurs within ~0.5 km of the modern ice margin on all sides of Coropuna (Fig. 9). These sharp-crested moraines are as much as 50 m in relief and exhibit steep proximal and distal slopes. Gravel and cobbles dominate the surfaces, with abundant angular boulders perched on or embedded in the crests.

Consistent with expected insolation, MELM values (Table 2, Fig. 8b) for north-facing glaciers are 5650–5775 m (mean 5722 ± 52 m; $n = 5$), whereas those for south-facing glaciers range from 5200 m to 5550 m (mean 5360 ± 118 m; $n = 7$). On the western flank, MELMs occur between 5565 and 5760 m (mean 5660 ± 85 m; $n = 4$), with the higher values on north-facing slopes. There are no east-flowing glaciers today, precluding an east-west comparison.

On Solimana, the upper limits of late-Holocene moraines occur at 5640 m and 5719 m in *Q.* Caño and 5530 m at the head of *Q.* Saca Chacay (Table 2; Fig. 5). Late-Holocene moraines on Firura are confined to the mountain's southern flank, where the small cirque glacier deposited conspicuous lateral and terminal ridges. The maximum elevation of the left lateral moraine is 5300 m (Table 2). The upper limit of the right lateral moraine is obscured by talus.

Toe-Headwall-Altitude-Ratio reconstructions

For comparison with the MELM data, we calculated snowline elevations on Coropuna and Firura for both the LGM and late-Holocene maximum using the THAR method and a set of ratios between 0.2 and 0.3. LGM results are given in Table 1 and late-Holocene results in Table 2. All THAR-based snowline elevations include ± 15 m, unless stated. For both the LGM and late Holocene, this method yielded snowlines that are significantly higher on Coropuna's northern flank than on the southern flank. Average LGM values (using various THAR ratios - shown in parentheses here) range from 5116 ± 91 m (0.25) to 5200 ± 88 m (0.3) on the north side ($n = 6$) and from 4663 ± 232 m (0.25) to 4772 ± 224 m (0.3) on the south flank ($n = 7$). Values for the west side range from 5001 ± 71 m to 5098 ± 66 m using ratios of 0.25 and 0.3, respectively.

Calculations of average late-Holocene snowlines on Coropuna exhibit the same north-south pattern, ranging from 5713 ± 48 m (0.25) to 5757 ± 52 m (0.3) ($n = 6$) on the north side, and from 5319 ± 139 m (0.25) to 5384 ± 136 m (0.3) ($n = 7$) on the south side. Similar reconstructions for the western aspect yielded average snowlines between 5596 ± 19 m (0.25) and 5652 ± 18 m (0.3) ($n = 2$).

Average THAR-based reconstructions for Firura yielded LGM snowlines of between 4812 ± 41 m (0.25) and 4858 ± 41 m (0.3) for the south side and between 4962 ± 37 m (0.25) and 4998 ± 37 m (0.3) for the north side. Late Holocene values for the south-facing cirque glacier range from 5275 ± 15 m (0.25) to 5289 ± 15 m (0.3).

Table 1. Last Glacial Maximum MELM, bifurcation, and THAR-calculated ELA values for the Pucuncho peaks.

Glacier	Terminus elevation (m)	Summit elevation (m)	MELM ELA (m)	THAR 0.25 ELA (m)	THAR 0.28 ELA (m)	THAR 0.3 ELA (m)
Coropuna (N)						
1	4830	6320	5150	5203	5247	5277
2	4730	6320	5230	5128	5172	5207
3 (L)	4540	6230	>5115	4963	5013	5047
3 (R)	4540	6230	>4930	4963	5013	5047
4	4630	6450	5120	5085	5139	5176
5	4790	6450	>4930	5205	5255	5288
6	4670	6450	>5040	5115	5168	5204
Average			5167 ± 59	5116 ± 91	5166 ± 89	5200 ± 88
Coropuna (W)						
7 (L)	4662	6450	4820	5109	5163	5198
7 (R)	4662	6450	4870	5109	5163	5198
8 (L)	4550	6450	4970	5025	5082	5120
8 (R)	4550	6450	>4850	5025	5082	5120
9	4460	6450	>4850	4958	5017	5057
10	4490	6450	>4730	4980	5039	5078
11	4430	6450	–	4935	4996	5036
Average			4887 ± 77	5001 ± 71	5059 ± 68	5098 ± 66
Coropuna (S)						
12	4370	6450	4700	4890	4952	4994
13	4545	6450	4790	5021	5078	5117
14	3917	6160	>4730	4478	4545	4590
15 (L)	3780	6230	>4650	4393	4466	4515
15 (R)	3780	6230	>4600	4393	4466	4515
16	4220	6230	>4590	4723	4783	4823
17 (L)	3900	6230	>4282	4483	4552	599
17 (R)	3900	6230	>4500	4483	4552	599
18	4100	6320	>4490	4655	4722	4766
Average			4745 ± 66	4663 ± 232	4728 ± 228	4772 ± 224
Solimana						
Q. Caño (L)	4530	6093	4980	–	–	–
Q. Caño (R)	4530	6093	5030	–	–	–
Unnamed (L)	4590	6093	4990	–	–	–
Unnamed (R)	4590	6093	5050	–	–	–
Q. Saca Chacay	5422	6093	~4850[a]	–	–	–
Firura						
North side	4783[b]	5498	>5000	4962	4983	4998
South side	4583[c]	5498	>4900	4812	4839	4858

(L) and (R) indicate left and right lateral moraines. Elevations marked with > refer to bifurcating moraines. [a] Snowline elevation calculated by Dornbusch (2002) using AAR of 0.67. [b] Averaged terminus elevation for northern flank. [c] Averaged terminus elevation for southern flank.

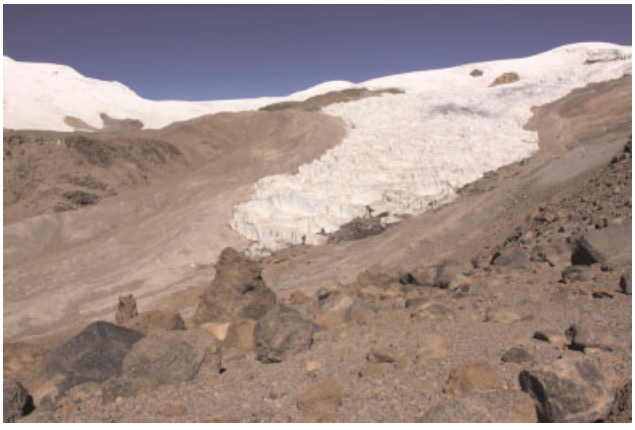

Figure 9. Late-Holocene moraines in front of Glacier 4, on the north side of Coropuna. This figure is available in colour online at wileyonlinelibrary.com.

Estimates of modern ELA on Coropuna

With significant glacier retreat over the last ~150 years, the overall magnitude of snowline rise at Coropuna since the LGM exceeds the LGM–late Holocene offset. However, measuring the change in snowline since the late Holocene maximum is complicated by ongoing recession (Meier *et al.*, 2003). At Coropuna, moraines being deposited along the retreating ice margins tend to be small (<1-2 m relief) and discontinuous in nature. Critically, these modern moraines are concentrated near the termini and do not form lateral ridges, thereby precluding use of the MELM method.

The THAR method also is inappropriate for resolving modern snowline elevations on Coropuna. As discussed below, THAR-derived snowlines for both the LGM and late-Holocene maximum are highly consistent with the MELM reconstructions when ratios between 0.2 and 0.3 are used (on average, 0.28 provides the closest match). However, calculations made using

Table 2. Late-Holocene (mid-19th century) MELM, bifurcation, and THAR-calculated values for the Pucuncho peaks.

Glacier	Terminus elevation (m)	Summit elevation (m)	MELM ELA (m)	THAR 0.25 ELA (m)	THAR 0.28 ELA (m)	THAR 0.3 ELA (m)
Coropuna (N)						
1	5584	6320	5775	5768	5790	5805
2	5458	6320	5705	5674	5699	5717
3	5466	6230	5762	5657	5680	5695
4	5438	6450	5650	5691	5721	5742
5	5530	6450	–	5760	5788	5806
6	5490	6450	5719	5730	5759	5778
Average			5722 ± 52	5713 ± 48	5740 ± 48	5757 ± 52
Coropuna (W)						
7	–	–	–	–	–	–
8 (L)	5320	6450	5626	5603	5636	5659
8 (R)	5320	6450	5760	5603	5636	5659
9	–	–	–	–	–	–
10 (L)	5300	6450	5565	5588	5622	5645
10 (R)	5300	6450	5690	5588	5622	5645
11	–	–	–	–	–	–
Average			5660 ± 85	5595 ± 19	5629 ± 18	5652 ± 18
Coropuna (S)						
12	5170	6450	5550	5490	5528	5554
13 (L)	5200	6450	5453	5513	5550	5575
13 (R)	5200	6450	5466	5513	5550	5575
14 W	4800	6450	5433	5213	5262	5295
14 E	4800	6160	5299	5140	5181	5208
15 (L)	4950	160	5290	5253	5289	5313
15 (R)	4950	160	5200	5253	5289	5313
16	5000	6230	>5290	5308	5344	5369
17	5010	6230	>5260	5315	5352	5376
18	–	–	–	–	–	–
Average			5384 ± 123	5319 ± 139	5358 ± 137	5384 ± 136
Solimana						
Q. Caño (L)	5460	6093	5640	–	–	–
Q. Caño (R)	5460	6093	5719			
Q. Saca Chacay	5395	6093	5530	–	–	–
Firura						
South side	5200	5498	5300	5275	5283	5289

(L) and (R) indicate left and right lateral moraines. Elevations marked with > refer to bifurcating moraines. Two glacier tongues occupying the same valley drainage are listed as 14W and 14E. In some valleys, such as 7 and 9, glaciers were absent during the late Holocene maximum.

these values result in modern snowline estimates that are far too low compared to published estimates of modern tropical glaciologic conditions. For example, on Coropuna's north flank, a THAR of 0.3 produces an average modern snowline of 5812 ± 53 m, which is only 55 m above the average late-Holocene snowline calculated for the same aspect and using the same ratio. Such a minor rise in snowline is incompatible with estimates from elsewhere in the tropics and higher latitudes (e.g. Haeberli, 1990; Kaser and Osmaston, 2002, and references therein; Mark and Seltzer, 2005; Rabatel *et al.*, 2006), most of which indicate significantly higher rates of snowline rise, and is also incompatible with the measured reduction in glacier area at Coropuna since the mid-20th century (Racoviteanu *et al.*, 2007).

For these reasons, and in the absence of published mass-balance data for the site, we used a combination of map-based ELAs and climate-model data to approximate modern snowlines on Coropuna. First, we located the inflection from convex (ablation zone) to concave (accumulation zone) on the glacier surface contours (e.g. Hess, 1904; Østrem, 1966; Porter, 1975; Fountain *et al.*, 1999). Leonard and Fountain (2003) termed this inflection point the kinematic ELA to distinguish it from the observed (measured) ELA, which can fluctuate significantly on an inter-annual basis. They also conducted the first empirical test of this map-based method, showing that the kinematic ELA provides a reasonable approximation of the observed snowline on a variety of glaciers, including the tropical Lewis Glacier on Mt. Kenya.

We identified the kinematic ELA on eleven outlet glaciers on Coropuna using the digital elevation model (DEM) of Racoviteanu *et al.* (2007). Their DEM was created using 1:50,000 topographic maps (Instituto Geográfico Nacional), based on 1955 aerial photographs, and verified with an extensive series of GPS field measurements. Vertical error in the DEM was evaluated by calculating root mean square errors with respect to a network of non-glaciated ground control points and is given as ± 23 m (Racoviteanu *et al.*, 2007). Correspondingly, our kinematic ELA determinations include this vertical uncertainty. ELA values are highest on north-flowing glaciers and lowest on south-flowing glaciers (Table 3), as reflected by the distribution of modern terminus elevations. Glaciers originating in broad saddles between domes (e.g. Glaciers 4 and 10) typically exhibit lower kinematic ELAs and terminus elevations than glaciers originating on the domes

Table 3. Palaeo- and modern ELA values for Coropuna's glaciers.

Glacier	MELM ELA_{LGM} (m)	MELM ELA_{IH} (m)	ELA_k (m)	Modern ELA (m)	ΔELA (m)
North aspect					
1	5150	5775	5860	5945	795
2	5230	5705	5840	5925	695
3 (L)	[5167 ± 59]	5762	5820	5905	738*
3 (R)	[5167 ± 59]	–	5820	5905	738*
4	5120	5650	5770	5855	735
5	–	–	–	–	–
6	[5167 ± 59]	5719	5860	5945	778*
Average	5167 ± 59	5722 ± 52	5830 ± 44	5915 ± 44	
West aspect					
7 (L)	4820	–	–	–	–
7 (R)	4870	–	–	–	–
8 (L)	4970	5626	5770	5855	885
8 (R)	[4887 ± 77]	5760	5770	5855	968*
9	–	–	–	–	–
10 (L)	[4887 ± 77]	5565	5700	5785	898*
10 (R)	[4887 ± 77]	5690	5700	5785	898*
11	–	–	–	–	–
Average	4887 ± 77	5660 ± 85	5735 ± 54	5850 ± 54	
South aspect					
12	4700	5550	–	–	–
13 (L)	4790	5453	–	–	–
13 (R)	–	5466	–	–	–
14 W	[4745 ± 66]	5433	5500	5585	840*
14 E	[4745 ± 66]	5299	5500	5585	840*
15 (L)	[4745 ± 66]	5290	5430	5515	770*
15 (R)	[4745 ± 66]	5200	5430	5515	770*
16	[4745 ± 66]	[5384 ± 123]	5550	5635	890*
17 (L)	–	–	–	–	–
17 (R)	–	–	–	–	–
18	–	–	–	–	–
Average	4745 ± 66	5384 ± 123	5495 ± 54	5580 ± 54	

LGM reconstructions (ELA_{LGM}) are from Table 1, late-Holocene data (ELA_{IH}) from Table 2. Kinematic ELA (ELA_k) values for eleven glaciers (reconstructions were not possible on all glaciers studied) are based on the DEM of Racoviteanu et al. (2007) and relevant to the long-term ELA ~1955. Estimates of modern ELA reflect the sum of ELA_k and ~85 m of snowline rise since ~1955 (based on temperature observations of Vuille et al. (2008) and a mean lapse rate 6.5°C/km). ΔELA represents the total difference in snowline altitude between the LGM and today (2010) for specific glaciers. Where ELA data were not available for a specific glacier/time, the appropriate aspect-average snowline value has been substituted (in square brackets) to enable calculation of ΔELA; asterisks (*) show the values calculated in this way.

themselves (e.g. Glaciers 1 and 6), potentially reflecting differences in accumulation.

These map-based measurements indicate that the mean kinematic ELA lies at 5830 ± 44 m on the north side of Coropuna and 5495 ± 54 m on the south side (Table 3), with a mean elevation of 5687 ± 49 m for the mountain. However, due to the age of the maps used to produce the DEM, the kinematic values given in Table 3 correspond to average glaciologic conditions in 1955, not the present. Assuming the lapse rate at Coropuna lies between 6 and 7°C/km (Klein *et al.*, 1999; Kaser and Osmaston, 2002), the 0.10°C per decade warming observed throughout the tropical Andes (Vuille *et al.*, 2008) is sufficient to have raised the snowline on Coropuna by an additional 80-90 m since 1955.

Discussion

LGM snowline depression in the Pucuncho region

The upper limit of moraines suggests the LGM snowline lay between ~5120 and 5230 m (mean 5167 ± 59 m; $n = 3$) on Coropuna's north side and between 4700 and ~4800 m (mean 4745 ± 66 m; $n = 2$) on the south side, and that an east-west snowline gradient existed on the mountain. Such gradients are common in tropical snowline reconstructions (Hastenrath, 2009), possibly reflecting enhanced sublimation on eastern flanks due to the prevailing airflow (Wright, 1983). These geomorphologic estimates for Coropuna are in broad agreement with the THAR reconstructions with ratios of 0.2–0.3. For example, a ratio of 0.28 produces average LGM snowlines of 5166 ± 89 m ($n = 6$) and 4728 ± 228 m ($n = 7$) for the north and south flanks, respectively (Table 1).

The largest discrepancy between the MELM and THAR methods occurs on Coropuna's western flank, where the average MELM value is ~100-200 m lower than the THAR calculations (Table 1). Considering the high degree of moraine preservation and consistent MELM values on this side of the mountain, we suggest that the THAR method overestimates the palaeo ELA to produce this offset. Unlike the MELM data, which are based solely on geomorphology, THAR calculations are based on an altitude range and therefore do not incorporate local factors, such as drifting or shielding by afternoon cloud cover (e.g. Kaser and Georges, 1997).

Moraine data from Coropuna's north side also compare well to MELM reconstructions for the north flank of Solimana, which

suggest LGM snowlines of 5013 ± 35 m ($n = 4$). Palaeo-snowlines on Solimana of ~5000 m elevation for north-facing *Q.* Caño and 4800-4850 m for south-east facing *Q.* Saca Chacay (Fig. 5) also were reconstructed by Dornbusch (2002) using an AAR of 0.67 and, though lacking age control, compare well to our geomorphic reconstructions. On Firura, moraine-based reconstructions are minimum values only, showing that LGM snowlines were no lower than ~5000 m on the north side and ≥4900 m on the south side. THAR-based snowlines, meanwhile, are slightly lower, ranging from 4962 m (0.25) to 4998 m (0.3) for the northern flank and from 4812 m (0.25) to 4858 m (0.3) on the south side (THAR shown in parentheses). The systematic differences between the two datasets indicate that the THAR method slightly underestimates snowline on Firura when ratios 0.2-0.3 are used. As discussed below, this disparity highlights the potential for error when a single ratio is used to reconstruct snowlines across a region.

MELM data indicate that the late-Holocene snowline on Coropuna was located between 5200 and 5775 m and, similar to today, exhibited a shallow gradient from north to south. THAR-based reconstructions are in close agreement (Table 2). Late-Holocene moraines on Solimana suggest snowline lay between 5680 m (north) and ~5530 m (south-east). Meanwhile, a single MELM measurement on Firura indicates that late-Holocene snowline occurred at ~5300 m on the south side. Again, THAR-derived values are slightly lower than the moraine data (Table 2). The absence of glacial deposits on the northern slope indicates the ELA either was too close to the summit for glacier growth or above the peak altogether.

Together, our MELM and THAR data indicate that LGM snowline in the Pucuncho region was significantly lower than during the late Holocene. According to the MELM-based reconstructions, the average offset on Coropuna was 555 ± 111 m for the north side, 639 ± 189 m for the south side, and 773 ± 162 m for the west side. By comparison, the averaged THAR data provide offset values of 574 ± 137 m for Coropuna's northern aspect and 630 ± 365 m for the southern aspect. On Solimana, the magnitude of snowline lowering relative was approximately 670 m and 680 m for the northern and south-eastern flanks, respectively. Farther north, LGM–late-Holocene snowline depression on Firura's south side was ≤400 m, according to moraine data, and 432 m based on a THAR of 0.3. These relatively low values likely reflect the influence of non-climatic factors on glacier response to climate.

To account for snowline rise since the late-Holocene maximum, we combined measurements of kinematic ELA on Coropuna and observed regional temperature data. Our kinematic reconstructions, corresponding to the 1950 s, provide snowline values of between 5430 m and 5860 m (mean 5691 ± 164 m) similar to those of Dornbusch (5613 m) (Dornbusch, 1998). We applied an additional 85 m elevation to our kinematic values to approximate modern (2010) snowline elevations, basing this value on the temperature dataset of Vuille *et al.* (2008) and a lapse rate of 0.65°C/100 m. While this is an estimate and not a site-specific value, it is the midpoint of a range of lapse rates (0.6-0.7°C/100 m) described by Kaser and Osmaston (2002) as being the most appropriate for this location and elevation. A lower rate of 0.6°C/100 m would increase our estimates of modern snowline by only ~5 m.

Combining these datasets allows us to approximate ELA rise on Coropuna since the mid-19th century. On average, the modern snowline is 193 ± 23 m higher on the north side, 160 ± 50 m on the west, and 248 ± 82 m higher on the south side than during the late Holocene. This pronounced snowline rise is consistent with the significant measured reduction in ice cover – approximately 26% – between 1962 and 2000 (Racoviteanu *et al.*, 2007). Significantly, we were unable to calculate similar values for modern snowlines using the THAR method and ratios of 0.2–0.3. Though this range produces LGM and late-Holocene snowlines that are consistent with MELM reconstructions, THAR-based modern estimates are, on average, ~100 m lower than the kinematic/lapse rate-derived values given in Table 3. For most glaciers investigated, it is necessary to employ ratios of 0.4-0.45 to produce comparable results.

This striking disparity highlights a limitation of ratio-based methods, namely that the same value used to calculate steady state ELA cannot be applied for non-steady state conditions (e.g. retreat). When reconstructing palaeo-ELAs it is widely assumed that the glacier was in, or near, a state of mass balance. However, while this assumption is valid for at least part of the LGM and the late-Holocene maximum, it is not valid for most tropical glaciers today. Owing to the response time of glaciers to climatic change, the onset of glacier retreat – and therefore any significant change in glacier-altitude range or area – will lag snowline rise by several years/decades (Johannesson *et al.*, 1989). When snowline rise is sustained, or accelerating, the vertical offset between terminus and ELA increases. Therefore, snowline rise on Coropuna due to sustained warming of at least the last sixty years (Vuille *et al.*, 2008) is outpacing terminus retreat, causing the THAR to shift from nearer steady state values to strongly negative ratios.

Collectively, the LGM and modern estimates approximate the overall magnitude of LGM snowline depression at Coropuna (Table 4). On the mountain's north side, the LGM snowline was approximately 748 ± 103 m lower than at present. On the southern flank this value is 835 ± 120 m and on the west side it is 963 ± 131 m. Together, these data produce an average ΔELA of ~850 m for the whole mountain. However, Mark *et al.* (2005) suggested that a closer estimate for a region is provided by the minimum ΔELA value in the range – in this case ~750 m. By choosing this value, we avoid basing our interpretations of the Coropuna snowline record on estimates that, because of localised, non-climatic effects, likely exaggerate the true magnitude of ΔELA. The relatively large offset on the west flank, for example, probably reflects the combined influence of drifting, topographic shading and shielding by clouds in addition to climate and, therefore, is an unsuitable basis for climatic interpretation.

Table 4. Snowline depression values for Coropuna, Solimana and Firura, including the LGM–late-Holocene offset ($\Delta ELA_{LGM\text{-}lH}$) and the overall LGM-modern ($\Delta ELA_{LGM\text{-}2010}$) offset.

	$\Delta ELA_{LGM\text{-}lH}$ (m)	$\Delta ELA_{LGM\text{-}2010}$ (m)
Coropuna		
North	555 ± 111	748 ± 103
West	773 ± 162	963 ± 131
South	639 ± 189	835 ± 120
Solimana		
North	667 ± 89	867 ± 89
South-east	~680	~880
Firura		
North	≥498	≥498
South	≤400	>400

Coropuna values incorporate aspect-averaged data from Table 3. Since MELM data are unavailable for the south-east flank of Solimana, we substituted the most conservative LGM snowline estimate of Dornbusch (2002). All $\Delta ELA_{LGM\text{-}2010}$ values for Solimana assume that modern snowline is ~200 m above late-Holocene estimates.

Assuming a similar degree of snowline rise (~200 m) on Solimana since the mid-19th century, the overall magnitude of ΔELA is approximately 800-900 m (Table 4). The broad consistency between Coropuna and Solimana, despite stark differences in topography, gives us confidence in our reconstruction of LGM snowline depression. However, on Firura a similar ~200 m rise in snowline would place the modern ELA above the summit of this currently glaciated peak, raising the following question: Is the Firura glacier sustained by an anomalously low ELA or is it a stagnant remnant, out of equilibrium with present climate?

All three peaks rise from the same plateau and are subject to the same climate, prevailing wind direction and insolation flux. Therefore, the apparent disparity in modern ELA is unlikely to be the result of variable climate parameters, such as precipitation. Nonetheless, different glaciers can experience locally variable rates of accumulation as a result of topographically controlled drifting. We consider this process improbable as the low relief and elevation of Firura are unlikely to result in significant input of drifting snow relative to Coropuna and Solimana. The subdued topography of Firura also precludes topographic shading and/or debris cover as factors influencing the modern ELA.

For the reasons discussed above, we consider it unlikely that the Firura glacier is being sustained by an anomalously low ELA. Instead, we suggest that the snowline has risen above the summit since the late-Holocene and, therefore, that the modern glacier is a remnant and out of equilibrium with present climate. This scenario is consistent with the occurrence of crater-like ablation features (10-20 m diameter, ~5 m deep) in the surface of the glacier and with modern ELA on the same aspect of Coropuna (Table 3). The remnant nature of the Firura glacier cautions against using smaller ice masses as indicators of modern snowline elevations, especially in dry, high-altitude settings where the ELA might occur several hundred metres above the 0°C isotherm. Such glaciers, once disconnected from the local snowline, might persist for a considerable time because ablation is dominated by sublimation and not by melting.

Assuming no change in precipitation and employing lapse rates between 6.0 and 7.0°C/km, our ΔELA values (748 m) from Coropuna translate to LGM temperature depressions of 4.5–5.2°C. A persistent issue in the interpretation of tropical snowlines is the relative contributions of temperature and precipitation to past glacial events. A traditional method for separating the two signals is to compare snowline data to local, independent records of precipitation (Seltzer, 1992). However, such precipitation records are unavailable for Coropuna at present. Moreover, existing precipitation reconstructions from southern Peru and northern Bolivia reveal significant variability, with some suggesting that LGM conditions were relatively dry (Servant and Fontes, 1978; Hansen *et al.*, 1984; Placzek *et al.*, 2006; Mourguiart and Ledru, 2003) and others that the glacial climate may have been wetter than at present (Hastenrath and Kutzbach, 1985; Servant *et al.*, 1995; Baker *et al.*, 2001; Thompson *et al.*, 2000; Chepstow-Lusty *et al.*, 2005; Hillyer *et al.*, 2009).

One possible approach to the problem is to model the response of glaciers to different climate scenarios, thereby producing a range of potential temperature-precipitation solutions (e.g. Kull and Grosjean, 2000; Anderson and Mackintosh, 2006). In the absence of long-term, local precipitation data, we are utilising this methodology to elaborate on the climatic implications of the Pucuncho snowline record. Currently, we are developing an energy mass-balance model that will simulate glacier behaviour at Coropuna.

Consistency and variability of late-Pleistocene snowline depression

The magnitude of LGM snowline lowering at Coropuna is broadly consistent with published reconstructions from some tropical sites. For example, Dornbusch (2002) reported that snowline was depressed by 675–800 m (relative to ~1955) throughout the Cordillera Ampato, southern Peru. Similarly, modelled reconstructions suggest that snowlines in the Coropuna region were depressed ~700 m during the LGM (Fox and Bloom, 1994; Klein *et al.*, 1999). In the Cordillera Blanca, northern Peru (9°S), Rodbell (1992) reported an average ΔELA of ~700 m. Beyond Peru, estimates of ΔELA from Ecuador (Clapperton, 1987), Colombia (Hoyos-Patiño, 1998), Mexico (White and Valastro, 1984), Hawaii (Porter, 1979), Kilimanjaro (Osmaston, 1989) and Mt. Kenya (Mahaney, 1990) fall within the range of 725-1120 m (Porter, 2001, and references therein).

An LGM snowline depression of ~750 m at Coropuna also is consistent with several estimates from higher-latitude sites. For example, Porter (1975) and McCarthy *et al.* (2008) calculated late-Pleistocene snowline depression of 750-875 m and 960 m, respectively, for the Southern Alps of New Zealand. Similar values have been reported from north-eastern China (>1000 m; Zhang *et al.*, 2008), Alaska (~700 m; Balascio *et al.*, 2005), Patagonia (900 m; Hubbard *et al.*, 2005) and the Rockies/Sierra Nevada (~800 m; Burbank, 1991), suggesting that the magnitude of LGM cooling was essentially uniform between at least parts of the tropics and higher latitudes.

Despite these similarities, tropical reconstructions are highly disparate over short distances (Mark *et al.*, 2005; Smith *et al.*, 2005b). For example, Wright (1983) reported values of 300-400 m for the central Peruvian Andes, while in the Bolivian Cordillera Real, Seltzer (1992) calculated ΔELA of 320–420 m. Mark *et al.* (2002) reported snowline lowering of only 150 m and 360 m for the Cordillera Vilcanota and Quelccaya Ice Cap, respectively, both located within 260 km of Coropuna and at a similar latitude (13.9°S; Fig. 1a). These inconsistencies may reflect either extreme regional climate variability (see Kull *et al.*, 2008) or different reconstruction methods (Porter, 2001; Benn *et al.*, 2005). Alternatively, site-specific environmental effects can cause local variability in glacier response (e.g. Mark *et al.*, 2005).

It is not the purpose of this paper to regurgitate the findings of several recent syntheses of tropical snowline data (e.g. Porter, 2001; Mark *et al.*, 2005; Smith *et al.*, 2005b, 2008). Nonetheless, the pattern of snowline evolution in the Pucuncho region showcases some of the mechanisms proposed to explain the variability in published ΔELA. For example, the magnitude of LGM snowline lowering relative to the late Holocene was significantly smaller on Firura than on Coropuna. In their study of regional snowline evolution, Klein *et al.* (1999) described how glaciers advancing onto low-relief, high-elevation terrain would exhibit smaller ΔELA values because further lowering of the snowline would have driven ice expansion horizontally, not vertically. Reconstructions of Pleistocene snowlines for such glaciers using altitude ratios would suggest only minor ΔELA simply because topography prevented ice reaching lower altitudes. This effect may explain some of the east-west asymmetry in snowline depression reported by Smith *et al.* (2005a) for sites in the Eastern Cordillera of Peru and Bolivia, calculated using the THAR method but attributed by them to orographic precipitation controls. At both locations, west-flowing glaciers encountered low-angled terrain whereas east-flowing glaciers were relatively unrestricted. Similarly, LGM termini occurred at higher elevations (~4500 m) on the west side of the Quelccaya Ice Cap (Mark *et al.*, 2002), where ice

advanced onto a plain, than on the steeper eastern side, where our initial investigations show glaciers descended as low as ~4200 m.

The influence of elevation-limiting topography on LGM glacier response is demonstrated clearly on the north side of Firura. There, ice was confined to a high plateau and only reached lower elevations where the glacier intercepted shallow drainages or the plateau edge. However, this effect does not account for the small ΔELA on the volcano's southern flank, where LGM glacier flow was unimpeded.

In a recent synthesis, Mark *et al.* (2005) reported a negative relationship between the magnitude of snowline depression and the elevation of the glacier headwall. Specifically, ΔELA values tend to be lower where headwall altitudes are greater. While this relationship clearly does not apply to the Pucuncho Basin, two mechanisms proposed by Mark *et al.* (2005) to explain their observed relationship might shed light on the cause of the anomalous Firura ΔELA. First, they suggested that a higher headwall equates to steeper glaciers. As a uniform drop in atmospheric snowline will produce a smaller mass-balance response for high-angled glaciers than for low-angled glaciers, the expected ΔELA of the former would be less than the latter despite a consistent forcing. However, although this mechanism might explain the low depression values reported for high-relief sites such as the Cordillera Vilcanota (Mark *et al.*, 2002), where glaciers are steep (Mercer and Palacios, 1977), it does not apply to Firura where relief generally is low. In contrast, Solimana exhibits high-angled slopes and steep glaciers, yet LGM snowline depression on that peak was substantial.

The second mechanism suggests that glaciers with smaller accumulation areas respond in a more muted fashion to climate than glaciers with large accumulation areas. As the accumulation area of the Firura glacier was significantly smaller than those on Coropuna and Solimana during both the LGM and late Holocene, this factor potentially accounts for at least part of the minor ΔELA on Firura. However, whereas Mark *et al.* (2005) argued that accumulation area decreases with increasing elevation, we suggest instead that the small accumulation area on Firura is a function of the peak's relatively low altitude and relief compared to Coropuna and Solimana.

In addition to these topographic considerations, other factors influencing the pattern of snowline change in the tropics are demonstrated by the Pucuncho record. First, retreating glaciers can exist in mountainous terrain for considerable time once the ELA has risen above the headwall/summit. Should these remnant ice fields then be used to indicate modern glaciologic conditions, ΔELA calculations will underestimate the true magnitude of change. As described above, this effect is most likely in dry, high-altitude settings, like the south-western Peruvian Andes. Nonetheless, a conservative approach would be to assume all reconstructions inferring modern ELA from small glaciers at or near the glaciation threshold (e.g. Wright, 1983) represent minimum ΔELA values only. This is particularly true for studies in which the reported 'modern' snowline actually corresponds to glaciologic conditions several decades ago (e.g. Ramage *et al.*, 2005).

A second factor potentially affecting tropical snowline measurements is the use of area/altitude ratios in determining modern ELA. As encountered on Coropuna, the correct THAR for reconstructing steady state conditions during the LGM is inappropriate for constraining modern snowlines. Consequently, we suggest that some of the variability in published ΔELA values for the tropics might be due to the same altitude or area ratios being used for palaeo and modern snowline reconstructions (e.g. Clapperton, 1987; Seltzer, 1992).

Similarly, a degree of variability is inevitable when reconstructions are based solely on assumed regional – as opposed to local – THAR or AAR values. For example, while ratios between 0.2 and 0.3 produced snowline estimates for Coropuna similar to the moraine data, these same ratios tended to underestimate slightly the ELA on Firura, both for the LGM and late-Holocene reconstructions. The magnitude of this uncertainty, though minor at Firura, can be significant if the chosen ratio is a regional average. For instance, in their reconstruction of late-Pleistocene snowline for the Quelccaya Ice Cap, Mark *et al.* (2002) employed a THAR to calculate a ΔELA of 360 m during the LGM. However, rather than incorporate a locally derived THAR, the authors used a ratio (0.45) based on regional snowline estimates for Peru, Bolivia and northern Chile (Klein *et al.*, 1999). Recalculated with a more appropriate ratio for such low-angled ice caps (e.g. 0.2-0.3), the magnitude of snowline depression at Quelccaya becomes significantly larger (~500-600 m).

The mechanisms and processes discussed here in the context of the Pucuncho record highlight methodological and non-climatic considerations likely influencing the consistency of tropical snowline reconstructions. Although critical re-evaluation of the existing dataset is beyond the scope of this paper, such scrutiny undoubtedly would reveal numerous instances where these and additional factors have led to artificially disparate ΔELA estimates. Nonetheless, as summarised by Mark *et al.* (2005), the variability displayed by the tropical database does not offset its value. For one, it is clear that late-Pleistocene snowline depression throughout much of the tropics was similar in magnitude to higher-latitude regions (Porter, 2001), demonstrating the broadly uniform nature of the global LGM. At the same time, several studies, verified by independent proxies, suggest that at least part of the range in tropical ΔELA represents patterns of real climate variability (e.g. Greene *et al.*, 2002; Blard *et al.*, 2009). Ultimately, accurate resolution of these patterns will afford the means to assess and characterise regional sensitivity of tropical glaciers to climate forcing. We reiterate the conclusions of Benn *et al.* (2005) in stressing that such resolution will depend in large part on the complete transparency of future snowline calculations.

Conclusions

Our reconstructions provide a measure of late-Pleistocene snowline depression from the Pucuncho region in the arid tropical Andes. In conjunction with the Coropuna chronology (Bromley *et al.*, 2009), this constitutes one of the first tropical snowline datasets dated unequivocally to the LGM. We used two separate methods – MELM and THAR – to generate palaeo-snowlines on Coropuna. Generally, the two datasets are in agreement and produce statistically similar values for LGM snowline lowering relative to the late Holocene.

The LGM on Coropuna was accompanied by snowline depression of ~555 m on the mountain's north side and ~640 m on the south side, relative to the late Holocene. Snowline lowering on neighbouring Solimana was of comparable magnitude but somewhat less on Firura. We suggest that this local variability reflects the influence of non-climatic effects on glacier behaviour at Firura. Accounting for the significant retreat of tropical glaciers since the mid-19th century, the overall magnitude of snowline rise on the north side of Coropuna since the LGM is approximately 750 m. This value is broadly consistent with higher-latitude sites and with the average magnitude of tropical ΔELA.

Our snowline reconstructions for Coropuna (~750 m) translate to a temperature depression of between 4.5 and 5.2°C during the LGM, assuming precipitation was similar to

today and using a range of lapse rates between 6 and 7°C/km. This value must be considered only a first-order estimate because of the possibility that precipitation also has varied in the past, and because of the inherent uncertainty associated with palaeo-snowline reconstructions.

Acknowledgements. Funding for the fieldwork was generously provided by the Dan and Betty Churchill Foundation, the Geological Society of America Graduate Student Research Grant programme, the Sigma Xi Grants-in-aid-of-research programme and the Comer Science and Educational Foundation. We thank Ben Gross, of Research Expedition Logistics, Utah, and Alexis Saénz Núñez de la Torre, of Peru 4x4, Arequipa, for logistical support and assistance in the field. We are grateful to Andrew Fountain, Aaron Putnam and Andrew Mackintosh for insightful discussions. We are particularly thankful to Eric Leonard and one anonymous reviewer, whose thorough comments greatly improved an earlier version of this manuscript.

Abbreviations. DEM, digital elevation model; ELA, equilibrium-line altitude; LGM, last glacial maximum; MELM, maximum elevation of lateral moraines; Q., Quebrada; THAR, toe-headwall-altitude-ratio.

References

Anderson B, Mackintosh A. 2006. Temperature change is the major driver of late-glacial and Holocene glacier fluctuations in New Zealand. *Geology* **34**: 121–124.

Andrews JT. 1975. *Glacial systems. An approach to glaciers and their environments*. North Scituate; Duxbury Press.

Asahi K, Watanabe T. 2004. Palaeoclimate of the Nepal Himalayas during the Last Glacial: reconstructing from equilibrium-line altitude. *Himalayan Journal of Science* **2**: 100–101.

Asahi K. 2008. Equilibrium-line altitudes of the present and Last Glacial Maximum in the eastern Nepal Himalayas and their implications of SW monsoon climate. *Quaternary International* **212**: 26–34.

Baker PA, Seltzer GO, Fritz SC, *et al*. 2001. The history of South American tropical precipitation for the past 25,000 years. *Science* **291**: 640–643.

Balascio NL, Kaufman DS, Manley WF. 2005. Equilibrium-line altitudes during the Last Glacial Maximum across the Brooks Range, Alaska. *Journal of Quaternary Science* **20**: 821–838.

Benn DI, Owen LA, Osmaston HA, *et al*. 2005. Reconstruction of equilibrium-line altitudes for tropical and sub-tropical glaciers. *Quaternary International* **138-139**: 8–21.

Blard P-H, Lave J, Farley KA, *et al*. 2009. Late local glacial maximum in the Central Altiplano triggered by cold and locally-wet conditions during the paleolake Tauca episode (17–15 ka, Heinrich 1). *Quaternary Science Reviews* **28**: 27–28.

Bromley GRM, Schaefer JM, Winckler G, *et al*. 2009. Relative timing of last glacial maximum and late-glacial events in the central tropical Andes. *Quaternary Science Reviews* **28**: 2514–2526.

Burbank DW. 1991. Late Quaternary snowline reconstructions for the southern and central Sierra Nevada, California and a reassessment of the ''Recess Peak Glaciation''. *Quaternary Research* **36**: 294–306.

Chepstow-Lusty A, Bush MB, Frogley MR, *et al*. 2005. Vegetation and climate change on the Bolivian Altiplano between 108,000 and 18,000 yr ago. *Quaternary Research* **63**: 90–98.

Clapperton CM. 1987. Maximal extent of late Wisconsin glaciation in the Ecuadorian Andes. *Quaternary of South America and Antarctic Peninsula* **5**: 165–179.

Clement AC, Cane MA, Seager R. 2001. An orbitally driven tropical source for abrupt climate change. *Journal of Climate* **14**: 2369–2375.

CLIMAP. 1981. *Seasonal reconstructions of the Earth's surface at the last glacial maximum*. Geological Society of America Map and Chart Series MC-36: Geological Society of America.

Dornbusch U. 1998. Current large-scale climatic conditions in southern Peru and their influence on snowline altitudes. *Erdkunde* **52**: 41–54.

Dornbusch U. 2002. Pleistocene and present day snowline rise in the Cordillera Ampato. *Neues Jahrbuch für Geologie und Paläontologie Abhandlungen* **225**: 103–126.

Fountain AG, Lewis KJ, Doran PT. 1999. Spatial climatic variation and its control on glacier equilibrium line altitude in TaylorValley, Antarctica. *Global and Planetary Change* **22**: 1–10.

Fox AN, Bloom AL. 1994. Snowline altitude and climate in the Peruvian Andes (5-17°S) at present and during the latest Pleistocene glacial maximum. *Journal of Geography* **103**: 867–885.

Greene AM, Seager R, Broecker WS. 2002. Tropical snowline depression at the Last Glacial Maximum: comparison with proxy records using a single-cell tropical climate model. *Journal of Geophysical Research* **107(D8)**: 4061. DOI: 10.1029/2001JD000670

Haeberli W. 1990. Glacier and permafrost signals of 20th century warming. *Annals of Glaciology* **14**: 99–101.

Hansen BCS, Wright HE, Bradbury JP. 1984. Pollen studies in the Junin area, central Peruvian Andes. *Geological Society of America Bulletin* **95**: 1454–1465.

Hastenrath S. 2009. Past glaciation in the tropics. *Quaternary Science Reviews* **28**: 790–798.

Hastenrath S, Kutzbach JE. 1985. Late Pleistocene climate and water budget of the South American Altiplano. *Quaternary Research* **24**: 249–256.

Hawkins F. 1985. Equilibrium-line altitudes and palaeoenvironments in the Merchants Bay area, Baffin Island, NWT, Canada. *Journal of Glaciology* **31**: 205–213.

Herreros J, Moreno I, Taupin J-D, *et al*. 2009. Environmental records from temperate glacier ice on Nevado Coropuna saddle, southern Peru. *Advances in Geosciences* **7**: 1–8.

Hess H. 1904. *Die Gletscher*. Braunschweig.

Hillyer R, Valencia BG, Bush MB, *et al*. 2009. A 24,700-yr paleolimnological history from the Peruvian Andes. *Quaternary Research* **71**: 71–82.

Hoyos-Patiño F. 1998. *Glaciers of Colombia*, In: *Satellite Image Atlas of Glaciers of the World – South America*. Williams RS Jr, Ferrigno JG (Eds.) USGS Professional Paper 1386-I, United States Government Printing Office: Washington, D.C; 11–30.

Hubbard A, Hein AS, Kaplan MR, *et al*. 2005. A modelling reconstruction of the Last Glacial Maximum ice sheet and its deglaciation in the vicinity of the Northern Patagonian Icefield, South America. *Geografiska Annaler* **87(A)**: 375–391.

Johannesson T, Raymond C, Waddington E. 1989. Timescale for adjustment of glaciers to changes in mass balance. *Journal of Glaciology* **35**: 355–369.

Kaser G, Georges C. 1997. Changes in the equilibrium line altitude in the tropical Cordillera Blanca (Peru) between 1930 and 1950 and their spatial variations. *Annals of Glaciology* **24**: 344–349.

Kaser G. 1999. A review of the modern fluctuations of tropical glaciers. *Global and Planetary Change* **22**: 93–103.

Kaser G, Osmaston H. 2002. *Tropical Glaciers*, International Hydrology Series; Cambridge; Cambridge University Press.

Klein AG, Seltzer GO, Isacks BL. 1999. Modern and last local glacial maximum snowlines in the central Andes of Peru, Bolivia and northern Chile. *Quaternary Science Reviews* **18**: 63–84.

Koutavas A, Lynch-Steiglitz J, Marchitto TM, *et al*. 2002. El Nino-like pattern in ice age tropical Pacific sea surface temperature. *Science* **297**: 226–297.

Kull C, Imhof S, Grosjean M, *et al*. 2008. Late Pleistocene glaciation in the Central Andes: Temperature versus humidity control- A case study from the eastern Bolivian Andes (17°S) and regional synthesis. *Global and Planetary Change* **60**: 148–164.

Kull C, Grosjean M. 2000. Late Pleistocene climate conditions in the north Chilean Andes drawn from a climate-glacier model. *Journal of Glaciology* **46**: 622–632.

Lachniet MS, Vazquez-Selem L. 2005. Last Glacial Maximum equilibrium line altitudes in the circum-Caribbean (Mexico, Guatemala, Costa Rica, Colombia and Venezuela). *Quaternary International* **138-139**: 129–144.

Leonard K, Fountain AG. 2003. Map-based methods for estimating glacier equilibrium line altitudes. *Journal of Glaciology* **49**: 329–336.

Licciardi JM, Schaefer JM, Taggart JR, *et al*. 2009. Holocene glacier fluctuations in the Peruvian Andes indicate northern climate linkages. *Science* **325**: 1677–1679.

Locke WW. 1990. Late Pleistocene glaciers and the climate of western Montana, USA. *Arctic and Alpine Research* **22**: 1–13.

Mahaney WC. 1990. *Ice on the Equator: Quaternary geology of Mount Kenya*. Wm Caxton Ltd.: Sister Bay.

Mark BG, Seltzer GO, Rodbell DT, *et al*. 2002. Rates of deglaciation during the Last Glaciation and Holocene in the Cordillera Vilcanota-Quelcaya Ice Cap region, southeastern Peru. *Quaternary Research* **57**: 287–298.

Mark BG, Harrison SP, Spessa A, *et al*. 2005. Tropical snowline changes at the last glacial maximum: A global assessment. *Quaternary International* **138-139**: 168–201.

Mark BG, Seltzer GO. 2005. Recent glacier recession in the Cordillera Blanca, Peru (AD 1962-1999). Spatial distribution of mass loss and climatic forcing. *Quaternary Science Reviews* **24**: 2265–2280.

McCarthy A, Mackintosh A, Rieser U, *et al*. 2008. Mountain Glacier Chronology from Boulder Lake, New Zealand, Indicates MIS 4 and MIS 2 Ice Advances of Similar Extent. *Arctic, Antarctic, and Alpine Research* **40**: 695–708.

Meier MF, Dyurgerov MB, Rick UK, *et al*. 2003. Glaciers Dominate Eustatic Sea-Level Rise in the 21st Century. *Science* **317**: 1064–1067.

Mercer JH, Palacios OP. 1977. Radiocarbon dating the last glaciation in Peru. *Geology* **5**: 600.

Meierding TC. 1982. Late Pleistocene glacial equilibrium-lines in the Colorado Front Range: a comparison of methods. *Quaternary Research* **18**: 289–310.

Mourguiart P, Ledru M-P. 2003. Last Glacial Maximum in an Andean cloud forest environment (Eastern Cordillera, Bolivia). *Geology* **31**: 195–198.

Munroe JS, Mickelson DM. 2002. Last Glacial Maximum equilibrium-line altitudes and paleoclimate, northern Uinta Mountains, Utah, U.S.A. *Journal of Glaciology* **161**: 257–266.

Osmaston H. 1975. Models for the estimation of firnlines of present and Pleistocene glaciers. In: *Processes in Physical and Human Geography*, Peel RF, Chisholm MDI, Haggett P (Eds.) Bristol Essays: Heinemann Educational: London; 218–245.

Osmaston HA. 1989. Glaciers, glaciations and equilibrium line altitudes on Kilimanjaro. In *Quaternary and Environmental Research on East African Mountains*, Mahaney WC (Ed.): Rotterdam: Balkema.

Østrem G. 1966. The height of the glaciation limi in southern British Columbia and Alberta. *Geografiska Annaler* **55**: 93–106.

Placzek C, Quade J, Patchett PJ. 2006. Geochronology and stratigraphy of late Pleistocene lake cycles on the southern Bolivian Altiplano: Implications for causes of tropical climate change. *GSA Bulletin* **118**: 515–532.

Pierrehumbert RT. 1999. Subtropical water vapour as a mediator of rapid climate change. *Geophysical Monograph* **112**: 339–361.

Pigati JS, Zreda M, Zweck C, *et al*. 2008. Ages and inferred causes of Late Pleistocene glaciations on Mauna Kea, Hawai'i. *Journal of Quaternary. Science* **23**: 683–702.

Porter SC. 1975. Equilibrium line altitudes of late Quaternary glaciers in the Southern Alps, New Zealand. *Quaternary Research* **5**: 27–47.

Porter SC. 1979. Hawaiian glacial ages. *Quaternary Research* **12**: 161–187.

Porter SC. 2001. Snowline depression in the tropics during the Last Glaciation. *Quaternary Science Reviews* **20**: 1067–1091.

Quade J, Rech JA, Betancourt JL, *et al*. 2008. Paleowetlands and regional climate change in the central Atacama Desert, northern Chile. *Quaternary Research* **69**: 343–360.

Rabatel A, Machaca A, Francou B, *et al*. 2006. Glacier recession on Cerro Charquini (16°S), Bolivia, since the maximum of the Lttle Ice Age (17th century). *Journal of Glaciology* **52**: 110–118.

Racoviteanu AE, Manley WF, Arnaud Y, *et al*. 2007. Evaluating digital elevation models for glaciologic applications:An example from Nevado Coropuna, Peruvian Andes. *Global and Planetary Change* **59**: 110–125.

Ramage JM, Smith JA, Rodbell DT, *et al*. 2005. Comparing reconstructed Pleistocene equilibrium-line altitudes in the tropical Andes of central Peru. *Journal of Quaternary Science* **20**: 777–788.

Rea BR, Whalley WB, Dixon TS, *et al*. 1999. Plateau icefields as contributing areas to valley glaciers and the potential impact on reconstructed ELAs: a case study from the Lyngen Alps, North Norway. *Annals of Glaciology* **28**: 97–102.

Rodbell DT. 1992. Late Pleistocene equilibrium-line reconstructions in the northern Peruvian Andes. *Boreas* **21**: 43–52.

Seltzer GO. 1992. Late Quaternary glaciation of the Cordillera Real, Bolivia. *Journal of Quaternary Science* **7**: 87–98.

Servant M, Fontes JC. 1978. Les lacs quaternaires des hauts plateaux des Andes boliviennes. Premières interpretations paléoclimatiques. *Cahiers O.R.S.T.O.M. Série Géoligie* **10**: 9–23.

Servant M, Fournier M, Argollo J, *et al*. 1995. La dernière transition glaciaire/interglaciaire des Andes tropicales sud (Bolivie) d'apres l'étude des variations des niveaux lacustres et des fluctuations glaciaires. *Comptes rendus de l'Académie des sciences* **320**: 729–736.

Smith JA, Seltzer GO, Farber DL, *et al*. 2005a. Early local last glacial maximum in the tropical Andes. *Science* **308**: 678–681.

Smith JA, Seltzer GO, Rodbell DT, *et al*. 2005b. Regional synthesis of last glacial maximum snowlines in the tropical Andes, South America. *Quaternary International* **138–139**: 145–167.

Smith JA, Mark BG, Rodbell DT. 2008. The timing and magnitude of mountain glaciation in the tropical Andes. *Journal of Quaternary Science* **23**: 609–634.

Solomina O, Jomelli V, Kaser G, *et al*. 2007. Lichenometry in the Cordillera Blanca, Peru: ''Little Ice Age'' moraine chronology. *Global and Planetary Change* **59**: 225–235.

Stansell ND, Polissar PJ, Abbott MB. 2007. Last glacial maximum equilibrium-line altitude and paleo-temperature reconstructions for the Cordillera de Mérida, Venezuelan Andes. *Quaternary Research* **67**: 115–127.

Thompson LG, Mosley-Thompson E, Davis ME, *et al*. 1995. Late Glacial Stage and Holocene ice core records from Huascarán, Peru. *Science* **269**: 46–50.

Thompson LG, Davis ME, Mosley-Thompson E, *et al*. 1998. A 25,000-Year Tropical Climate History from Bolivian Ice Cores. *Science* **282**: 1858–1864.

Thompson LG, Mosley-Thompson E, Henderson KA. 2000. Ice-core palaeoclimate records in tropical South America since the Last Glacial Maximum. *Journal of Quaternary Science* **15**: 377–394.

Thouret J-C, Wörner G, Gunnell Y, *et al*. 2007. Geochronologic and stratigraphic constraints on canyon incision and Miocene uplift of the central Andes in Peru. *Earth and Planetary Science Letters* **263**: 151–166.

Venturelli G, Fragipane M, Weibel M, *et al*. 1978. Trace element distribution in the Cainozoic lavas of Nevado Coropuna and Andagua Valley, Central Andes of southern Peru. *Bulletin of Volcanology* **41**: 213–228.

Vuille M, Francou B, Wagnon P, *et al*. 2008. Climate change and tropical Andean glaciers: Past, present and future. *Earth-Science Reviews* **89**: 79–96.

White SE, Valastro S. 1984. Pleistocene glaciation of volcano Ajusco, central Mexico, and comparison with the Standard Mexican glacial sequence. *Quaternary Research* **21**: 21–35.

Wright HE. 1983. Late Pleistocene climate and glaciation around the Junin Plain, central Peruvian Highlands. *Geografiska Annaler* **65(A)**: 35–43.

Zech R, Kull C, Kubik PW, *et al*. 2007. LGM and Late Glacial glacier advances in the Cordillera Real and Cochabamba (Bolivia) deduced from ^{10}Be surface exposure dating. *Climate of the Past* **3**: 623–635.

Zech R, May J-H, Kull C, *et al*. 2008. Timing of the late Quaternary glaciation in the Andes from ~15 to 40°S. *Journal of Quaternary Science* **23**: 635–647.

Zhang W, Cui Z, Yan L. 2008. Present and late-Pleistocene equilibrium line altitudes in Changbai Mountains, northeast China. *Journal of Geographical Sciences* **19**: 373–383.